Macromolecules

Article

pubs.acs.org/Macromolecules

How Does DNA Complex with Polyethylenimine with Different Chain Lengths and Topologies in Their Aqueous Solution Mixtures?

Zhuojun Dai[†] and Chi Wu*[,†,‡]

[†]Department of Chemistry, The Chinese University of Hong Kong, Shatin, N.T., Hong Kong

[‡]The Hefei National laboratory of Physical Science at Microscale, Department of Chemical Physics, The University of Science and Technology of China, Hefei, Anhui 230026, China

Supporting Information

ABSTRACT: Complexation between DNA with anionic charges (P) and polyethylenimine (PEI) with cationic charges (N) in aqueous solution condenses DNA into small insoluble aggregates (polyplexes), facilitating its delivery into cells. The study of the captioned problem is long overdue. Using a combination of static and dynamic laser light scattering, we showed that for a given topology PEI with a high molar mass is more effective in condensing DNA, while for a given molar mass, linear chains are more efficient in neutralizing DNA than their branched counterparts. The resultant polyplexes become stable when N/P $\geq$ 6 and, quantitatively, on average contain only one DNA. The ratio of gyration to hydrodynamic radii decreases after the DNA and PEI complexation but increases with the N/P ratio. This study reveals that linear chains can align themselves on DNA to effectively neutralize its anionic charges so that DNA collapses in water mainly due to its insolubility like a neutral hydrocarbon chain, while cationic branched chains condense each DNA chain mainly by pulling its intrachain anionic segments together and coat its periphery to form a mushroom-like PEI shell. Such two different condensation ways are supported by the results of adding strong polyanions (dextran sulfate, DS) into the polyplexes dispersion; namely, DS can ripe linear chains away from each polyplex layer by layer, like peeling an onion, to completely release DNA, but mostly strip cationic branched chains coated on the periphery, not those inside, to partially release DNA.

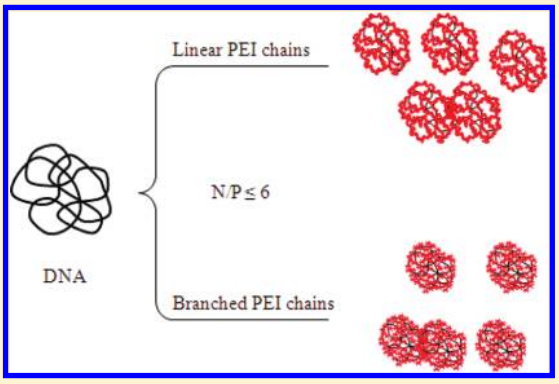

INTRODUCTION

The development of nonviral vectors to deliver DNA into cell nucleus has attracted much attention in the past few decades due to its less toxicity, easy modification, facial preparation, and storage, to name but a few.[1,2] Cationic synthetic polyelectrolytes (polycations) are one of the choices, and their complexation with anionic DNA chains has led to various *in vitro* nonviral vectors (polyplexes).[3] Among them, cationic polyethylenimine (PEI) is one of the commercial polymers tested in the earlier stage but still remains as one of the most effective nonviral vectors, especially for PEI chains with a molar mass higher than $\sim 10^4$ g/mol, in spite of its high cytotoxicity.[4−6] It is often cited in the literature that cationic amino groups (N) in PEI bind to anionic phosphate acid groups (P) in DNA via electrostatic attraction to neutralize charges on them so that DNA is condensed into individual stable aggregates, facilitating its endocytosis and providing a protection against enzymatic degradation before it enters the cell nucleus.[7,8] However, such a citation is inaccurate because the complexation is actually driven by the gain of translational entropy, namely, the releasing of counterions, instead of the gain of enthalpy via electrostatic interaction.[9]

In our scope of knowledge, detailed microscopic pictures of how the polyplexes are formed between DNA and cationic polymers with different topologies and chain lengths is still missing even though such polyplexes have been extensively prepared and used in the past 30 years with hundred thousands of publications. Partially, this is because their complexation is rather complicate. On the one hand, it is influenced by the degree of protonation of cationic chains with different kinds of amines. On the other hand, the chain flexibility, topology, and length of a chosen polymer also play important rules, especially because plasmid DNAs are semirigid chains with a persistent length of ~50 nm, much longer than ~1 nm for most of linear flexible neutral polymer chains in organic solvents or polyelectrolytes chains in water with salts.[10]

PEI with two different topologies, linear and branched, have been used in the gene delivery and transfection studies.[6,11,12] Linear PEI (LPEI) is composed solely of secondary amines except one primary amine end, while branched PEI (BPEI) includes primary, secondary, and tertiary amines with a ratio of ~1:2:1, as schematically shown in Scheme 1. The polyplexes made of different PEIs result in different physical properties and gene transfection efficiency. Previously, the polyplexes made of

Received: December 27, 2011
Revised: April 23, 2012
Published: May 8, 2012

Scheme 1. Schematic of Structures of Linear and Branched PEI Chains

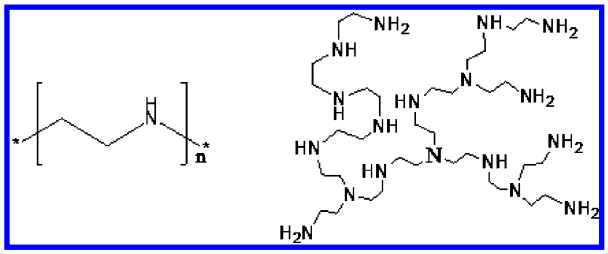

PEI with different chain lengths and topologies were extensively used in *in vitro* gene transfection studies, and significantly different transfection efficiencies were observed.[13−16] On the other hand, physical properties of PEI/DNA polyplexes have also been characterized by various methods, including circular dichroism, time-resolved fluorescence, and light scattering spectroscopies.[17−19] However, some basic problems are still unsolved. For example, how many DNA chains are inside each polyplex at different N/P ratios, how do the chain length and topology affect the final polyplexes structure, and how does such a structure difference influence the final gene transfection efficiency?

It has been generally known that when the N/P ratio reaches ∼3, no free DNA is detectable in gel electrophoresis, indicating that most of DNA chains are condensed by PEI.[20−22] Under this condition, the polyplexes formed in the solution mixture are unstable and tend to further aggregate because there is no sufficient amount of charges on their periphery to stabilize them. Further addition of PEI to N/P $\geq$ 6 stabilizes the resultant PEI/DNA polyplexes. At higher N/P ratios, only a portion of PEI chains are complexed with DNA, and the rest exist as individual chains free in the solution mixture, which was first revealed by Wagner and co-workers[23] and recently confirmed by Yue et al.[8] To facilitate the endocytosis and protect DNA from the enzymatic degradation, we like to condense and bind DNA with cationic polymer chains as strong as possible,[7,16,24,25] while inside the cytosol and especially inside the nucleus we would like to have an easy unloading of DNA from each polyplex.[26,27] Therefore, a delicate balance between being condensed in the extracellular space (and the cytosol) and being released in the nucleus is crucial for successful gene transfection.[28] Previously, we focused on how different LPEI/DNA and BPEI/DNA polyplexes perform in *in vitro* gene transfection[29] and how free PEI chains promote the gene transfection.[8] During these studies, we realized that there has been no systematic study on the detailed structure of the polyplexes with different N/P ratios in the solution mixtures, such as how many DNA chains inside each polyplexes, even thought there are some X-ray studies about the arrangements of the precipitated polyplexes.

In the current study, we focused on physical properties of different PEI/DNA polyplexes, such as their structures, complexation kinetics, and condensation mechanism, by using a combination of static and dynamic laser light scattering (LLS). In addition, we also used the polyanion exchange assay to measure the binding strength of different PEI chains with DNA inside the polyplexes. Our ultimate objective is to have a better understanding at microscopic level how cationic PEI with different topologies and chain lengths are complexed with and condense anionic DNA chains so that we can uncover possible correlation between their physical characteristics and the gene transfection efficiency.

MATERIALS AND EXPERIMENTS

Materials. Linear PEI samples with a weight-averaged molar mass (M_w) of 2.5 and 25 kg/mol (L2.5K and L25K) and branched PEI samples with M_w = 2.0 and 25 kg/mol (B2.0k and B25k) were purchased from Sigma-Aldrich and used without further purification. A high quality supercoiled plasmid DNA:pCMV-LUC (sequence available upon request, 5400 bp) was prepared using the endofree Maxi kit from Qiagen GmbH (Hilden, Germany) according to the manufacturer's instructions. Picogreen and dextran sulfate (DS, M_w = 10^4 g/mol) were respectively purchased from Invitrogen and Sigma-Aldrich.

Preparation of PEI/DNA Polyplexes. The N/P ratio is defined as the molar ratio of the nitrogen atoms in PEI to the phosphorus atoms in DNA double helix in the solution mixture. It should be emphasized that the N/P ratio is not the nitrogen/phosphorus ratio inside each polyplexes because some of PEI chains are free in the solution mixture even at lower N/P ratios. For the picogreen assay and gel electrophoresis, the polyplexes with a series of N/P ratios were prepared by adding a cationic PEI solution with different concentrations to an equal volume of a DNA solution with a fixed DNA content. Each resultant solution mixture was first gently vortexed for ∼5 s and then incubated for 10 min at room temperature before further studies. For LLS investigation, 10 μL of DNA solution with different amounts of DNA (0.5, 1.0, 1.5, or 2.0 μg) was added into a cylindrical light scattering cell with 0.5 mL of dust-free water. Afterward, 10 μL of dust-free PEI solutions with different concentrations were respectively added to achieve desired N/P ratios. The PEI and DNA aqueous solutions were gently mixed to ensure their complexation before it was characterized by LLS.

Complexation and Binding Strength between DNA and PEI. The complexation between DNA and PEI was evaluated using gel electrophoresis. The DNA and PEI solution mixtures were prepared as described above. Each DNA and PEI solution mixture with a desired N/P ratio was loaded on a 1% (w/v) agarose gel containing ethidium bromide (Biotium, Hayward, CA) in tris-borate EDTA buffer. The amount of DNA loaded into each well was 0.2 μg in a total volume of 10 μL. The electrophoresis was performed at 120 V for 30 min. DNA bands were visualized under UV. On the other hand, the complexation between DNA and PEI was quantified from the fluorescence quenching extent of picogreen that shows its maximum fluorescence intensity when intercalating with DNA; namely, the concentration of those uncomplexed DNA segments and chains free in the solution mixture can be quantitatively determined with a proper calibration. In practice, the fluorescence intensity of each solution mixture was measured 10 min after the addition of picogreen by using a plate reader (Hitachi F-7000, λ_{ex} = 480 nm, λ_{em} = 520 nm).

To study the binding strength between DNA and PEI in the polyplexes, long and strong polyanionic chains (dextran sulfate, DS) with a weight ratio of DS:DNA = 50:1 was added to each solution mixture and incubated for 30 min at room temperature. The binding strength between DNA and PEI was evaluated from the bands of DNA chains replaced and released by DS in electrophoresis. Moreover, the picogreen fluorescence assay described before was also used to quantitatively determine the extent of DNA replaced and released by DS from the polyplexes in the solution mixture.

Laser Light Scattering (LLS). A commercial LLS spectrometer (ALV/DLS/SLS-5022F) equipped with a multi-τ digital time correlator (ALV5000) and a cylindrical 22 mW He−Ne laser (λ_0 = 632 nm, Uniphase) was used. The incident beam was vertically polarized with respect to the scattering plane. The details of the LLS instrumentation and theory can be found elsewhere.[30−32] Briefly, in static LLS, the excess absolute time-averaged scattered light intensity of a dilute solution or dispersion, known as the excess Rayleigh ratio $R_{vv}(\theta)$, at a given polymer concentration (C) and a relatively low scattering angle (θ) is approximately related to the weight-average

dx.doi.org/10.1021/ma2027963 | *Macromolecules* 2012, 45, 4346−4353

molar mass (M_w), the square average radius of gyration ($\langle R_g^2 \rangle$), and the second virial coefficient (A_2) as

$$\frac{KC}{R_{vv}(\theta)} \approx \frac{1}{M_w}\left(1 + \frac{1}{3}\langle R_g^2\rangle q^2\right) + 2A_2C \quad (1)$$

where $K = 4\pi^2 n^2 (dn/dC)^2/(N_A \lambda_0^4)$ with N_A and dn/dC the Avogadro number and the specific refractive index increment, respectively, and $q = 4\pi n \sin(\theta/2)/\lambda_0$, where θ is the scattering angle. In dynamic LLS, each measured $G^{(2)}(q,t)$ is related to the normalized electric field−field time correlation function $g^{(1)}(q,t)$ by[30]

$$G^{(2)}(q, t) = A[1 + b|g^{(1)}(q, t)|^2] \quad (2)$$

where A is a baseline; $0 \le b \le 1$, a spatial coherent factor, depending on the instrumental detection optics. The value of b actually reflects the signal-to-noise ratio of a dynamic LLS measurement. It has been shown that $|g^{(1)}(q,t)|$ is proportional to $S(q,t)$ and related to the characteristic line-width distribution $G(\Gamma)$ by[30]

$$g^{(1)}(q, t) = \int_0^\infty G(\Gamma)e^{-\Gamma t}\, d\Gamma \quad (3)$$

The Laplace inversion of each measured $G^{(2)}(q,t)$ leads to one $G(\Gamma)$ based on eqs 2 and 3. The CONTIN algorithm in the digital time correlator was used.[33] For a pure diffusive relaxation, $G(\Gamma)$ can be converted into a translational diffusion coefficient distribution $G(D)$ by $D = \Gamma/q^2$ or further to a hydrodynamic radius distribution $f(R_h)$ by using the Stokes−Einstein equation.

RESULTS AND DISCUSSION

It has been manifested by previous results that mixtures of a DNA and a PEI aqueous solution are unstable and resultant polyplexes tend to further aggregate and precipitate when N/P ~ 3 even in a salt-free aqueous solution, presumably because there is no sufficient charge on their periphery to stabilize them. The aggregation mostly happens when negative charges on DNA are just neutralized by a sufficient amount of positive charge on PEI chains. It is worth noting that for small electrolytes coacervates or precipitates occur when the 1:1 charge stoichiometry is reached. However, it takes a ratio of N:P ~ 3 to condense DNA, presumably due to the imperfect matching of the cationic groups on PEI to the anionic groups on DNA and also due to the fact that not every amide group is protonized. Further addition of cationic chains dissolves the coacervates or precipitates even at salt-free conditions. As discussed before, such complexation has been frequently attributed to electrostatics interaction (enthalpy), but the actual underlining driving force is the gain of translational entropy due to the releasing of counterions from both DNA and PEI.[9] It is expected that the stabilization of the polyplexes made of different PEI chains would be highly related how they interact with DNA.

Note that in LLS the time average scattered light intensity ($\langle I \rangle$) of a given solution or dispersion is directly related to the molar mass (M) of a scattering object as follows:

$$\langle I \rangle \propto \sum_{i=1}^{N} W_i M_i \text{ or } \sum_{i=1}^{N} N_i M_i^2 \quad (4)$$

where W and N are the weight and number concentrations, respectively, which clearly shows that objects with a higher M scatter more light; in other words, LLS is much more sensitive to long DNA chains and large polyplexes than individual PEI chains in the solution mixture.

Figure 1 shows the time-dependent normalized scattered light intensity of mixtures of DNA and linear PEI (L2.5k and L25k) aqueous solutions for N/P = 3 but different initial DNA concentrations. No further polyplexes aggregation occurs when C_{DNA} is lower than 1 μg/mL, independent of the chain length. Note that the inter-polyplexes aggregation starts at higher DNA concentrations. Also note that the L2.5k/DNA polyplexes aggregate more than the L25k/DNA polyplexes, reflecting in their higher average aggregation number. We will explain it later after comparing their structures. When it comes to branched PEI chains, we observed no inter-polyplexes aggregation for small branched PEI chains until N/P reaches 4, while for large branched chains, the aggregation occurs only for higher DNA concentrations at N/P = 3, as shown in Figure 2, indicating the polyplexes made of branched chains are more stable.

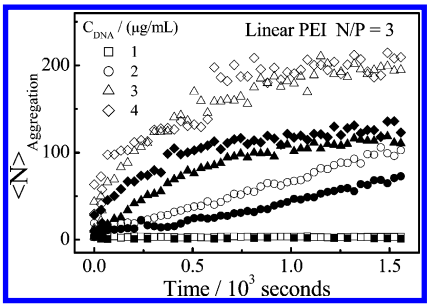

Figure 1. Time dependence of average number of DNA chains per polyplexes in different aqueous solution mixtures, where hollow and solid symbols represent L2.5k/DNA and L25k/DNA polyplexes, respectively.

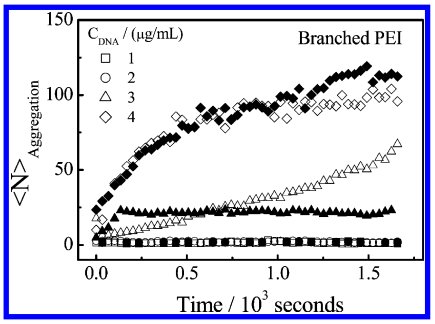

Figure 2. Time dependence of average number of DNA chains per polyplexes in different aqueous solution mixtures, where hollow and filled symbols represent B2.0k/DNA (N/P = 4) and B25k/DNA (N/P = 3), respectively.

It was previously shown that in the physiological pH range (6.5−10.0) the buffer capacities of PEI with different topologies are marginally different;[34,35] namely, both linear and branched PEI chains have a similar protonation ability. Therefore, it must be the difference in their three-dimensional structures that plays a critical role. Judging from their structures, linear cationic PEI chains can anneal with an anionic DNA chain easier and better and wrap around itself around DNA, while a DNA chain would have to bend and wrap itself on a branched PEI chain in order to make its anionic groups interact with all the cationic groups on PEI, which is unlikely because plasmid DNA is a semirigid chain with a persistent length of ~50 nm.[36,37] More likely, one side of each branched PEI chain would just bind to one segment of DNA and the other side to another distant intrachain segment or one segment on another DNA chain.

When N/P ≥ 6, the resultant polyplexes are stable and the scattered light intensity remains a constant over a long time (not shown). Assume that, on average, m PEI chains are complexed with each DNA chain. For the polyplexes with only

dx.doi.org/10.1021/ma2027963 | Macromolecules 2012, 45, 4346−4353

one DNA chain, $M_{1,polyplexes} = M_{DNA} + M_{PEI}m$. Further, inside the polyplexes, the weight fractions of DNA and PEI are as follows:

$$W_{DNA} = \frac{M_{DNA}}{M_{DNA} + M_{PEI}m} \text{ and } W_{PEI} = \frac{M_{PEI}m}{M_{DNA} + M_{PEI}m} \quad (5)$$

The differential refractive index increment of the polyplexes follows the additive rule, i.e.

$$\left(\frac{dn}{dC}\right)_{polyplexes} = W_{DNA}\left(\frac{dn}{dC}\right)_{DNA} + W_{PEI}\left(\frac{dn}{dC}\right)_{PEI} \quad (6)$$

where $(dn/dC)_{DNA} = 0.17$ mL/g and $(dn/dC)_{PEI} = 0.21$ mL/g in water.[38] LLS theory shows that

$$\langle I\rangle_{polyplexes} \propto \left(\frac{dn}{dC}\right)^2_{polyplexes} \sum_{i=1}^{N} C_{i,polyplexes}M_{i,polyplexes} \quad \text{(after complexation)} \quad (7)$$

$$\langle I\rangle_{DNA} \propto \left(\frac{dn}{dC}\right)^2_{DNA} C_{DNA}M_{DNA} \quad \text{(before complexation)} \quad (8)$$

where $C_{i,polyplexes}$ and $M_{i,polyplexes}$ ($= iM_{1,polyplexes}$) are the weight concentration and molar mass of the polyplexes containing i DNA chains, respectively. Hereafter, when $i = 1, 2, ..., n$, we call the polyplexes as unimer, dimer, ..., n-mer, respectively. The right sides of eqs 7 and 8 are measurable in static LLS. Experimentally, the polyelectrolytes effect leads two relaxation modes in dynamic LLS and the scattering intensity does not reflect that from individual DNA chains so that a proper amount of salt has to be added to suppress such an effect; namely, $\langle I\rangle_{DNA}$ should be the scattered light intensity after the addition of salt (as shown in the Supporting Information). The detailed discussion is beyond the scope of the current study. The ratio of the right sides of eqs 7 and 8 leads to

$$\frac{\langle I\rangle_{polyplexes}}{\langle I\rangle_{DNA}}\left(\frac{dn}{dC}\right)^2_{DNA} C_{DNA}M_{DNA} = \left(\frac{dn}{dC}\right)^2_{polyplexes} \sum_{i=1}^{N} C_{i,polyplexes}M_{i,polyplexes} \quad (9)$$

Assuming that all the polyplexes contain only one DNA chain, eq 9 can be rewritten as

$$\frac{\langle I\rangle_{polyplexes}}{\langle I\rangle_{DNA}}\left(\frac{dn}{dC}\right)^2_{DNA} C_{DNA}M_{DNA} = \left(\frac{dn}{dC}\right)^2_{polyplexes} C_{polyplexes}M_{1,polyplexes} \quad (10)$$

where the only unknown parameter "m" can be numerically determined. If all the PEI chains are attached to the DNA chains in the solution mixture, we can calculate "m_{max}" from the initial concentrations of DNA and PEI. In principle, m should not be larger than m_{max}. Whenever $m > m_{max}$, our previous all-unimer assumption must be wrong so that we have to consider further aggregation among the resultant polyplexes. In a very dilute solution mixture, it is reasonable to further assume that only polyplexes dimers were formed because of a rather limited increase in the scattering intensity and its weight content is x_w ($= W_{dimer}/W_{polyplexes}$). In this way, eq 10 can be rewritten as

$$\frac{\langle I\rangle_{polyplexes}}{\langle I\rangle_{DNA}}\left(\frac{dn}{dC}\right)^2_{DNA} C_{DNA}M_{DNA} = \left(\frac{dn}{dC}\right)^2_{polyplexes} [C_{polyplexes}(1 - x_w)M_{1,polyplexes} + C_{polyplexes}x_wM_{2,polyplexes}] \quad (11)$$

where $M_{2,polyplexes} = 2M_{1,polyplexes}$ and the only unknown parameter x_w can also be numerically found. Note that the number content of dimers (x_n) is related to x_w as $x_n = x_w/(2 - x_w)$.

Table 1 summarizes various calculated parameters from scattered light intensities of pure DNA and different DNA/PEI polyplexes in very dilute solution mixtures ($C_{DNA} = 1$ μg/mL). In Table 1, $m_{PEI,max}$ represents the maximum average number of PEI chains per DNA chain, calculated from the initial feeding N/P ratio. m_{PEI} is the actual value obtained from LLS measurements. Table 1 shows that in some cases m_{PEI} is larger than its corresponding $m_{PEI,max}$, indicating the formation of some inter-polyplexes aggregates, presumably, most of them are dimers in such a dilute solution mixture. We can estimate the dimer content (x_w and x_n) using eq 11, as shown in Table 1. The assumption is rational and reasonable because the addition of more PEI chains (up to N/P = 6) practically stabilizes individual resultant polyplexes so that each polyplex on average contains only one DNA chain. Previously, we quantitatively determined that ~2/3 of PEI chains are free in the solution mixture when N:P = 10.

Table 1. Parameters of Various PEI/DNA Polyplexes in Different Solution Mixtures[a]

					dimer content/%	
$(N/P)_{feed}$	sample	$m_{PEI,max}$	$\langle I\rangle_{polyplexes}/\langle I\rangle_{DNA}$	m_{PEI}	x_n	x_w
3	*l*PEI-2.5k	557	2.43	759	14	25
	*l*PEI-25k	56	2.06	60	2	4
	*b*PEI-2.0k	696	2.27	862	9	16
	*b*PEI-25k	56	2.30	71	10	18
6	*l*PEI-2.5k	1114	2.72	879	0	0
	*l*PEI-25k	112	2.82	92	0	0
	*b*PEI-2.0k	1392	3.33	1387	0	0
	*b*PEI-25k	112	3.62	122	0	0
10	*l*PEI-2.5k	1857	2.78	902	0	0
	*l*PEI-25k	187	2.68	87	0	0
	*b*PEI-2.0k	2321	3.13	1295	0	0
	*b*PEI-25k	187	3.91	132	0	0
12	*l*PEI-2.5k	2228	2.68	862	0	0
	*l*PEI-25k	224	2.89	95	0	0
	*b*PEI-2.0k	2785	2.88	1177	0	0
	*b*PEI-25k	224	3.41	114	0	0
15	*l*PEI-2.5k	2785	3.32	1106	0	0
	*l*PEI-25k	280	2.95	97	0	0
	*b*PEI-2.0k	3481	3.46	1445	0	0
	*b*PEI-25k	280	3.84	129	0	0

[a]Relative errors of these parameters: <*I*>, ±2%; m_{PEI}, ±5%; and x_n and x_w, ±10%.

Table 1 shows that at a relatively low concentration the inter-polyplexes aggregation still exists when N/P is low, presumably, the majority of PEI chains are bound to DNA, not free in the solution mixture; while for higher N/P ratios, $m_{PEI} < m_{max}$,

dx.doi.org/10.1021/ma2027963 | Macromolecules 2012, 45, 4346–4353

revealing that some of PEI chains are free in the solution mixture. In details, when N/P = 3, polyplexes in the solution mixture may contain more than one DNA chain, depending on the topology and chain length of PEI used. Two following possible ways are accounted for such inter-polyplexes aggregation. In the first pathway, some of DNA chains are fully neutralized by PEI with its local cationic/anionic ratio close to one so that they become insoluble in water, just like neutral hydrocarbon polymer chains, and tend to aggregate with each other to minimum their surface energy; while in the second pathway, some of PEI chains bind ("bridge" or "cross-linking") two segments on different DNA chains to induce the inter-polyplexes aggregation.

For linear PEI, shorter chains lead to more inter-polyplexes aggregates than longer ones. In an extreme case, small cationic amines (could be viewed as very short "chains") can neutralize anionic charges on DNA at N/P = 1, resulting in visible macroscopic precipitation. As expected, short chains have a lower entropic barrier to align themselves on a DNA chain and more effectively neutralize its anionic charges than long ones, leading to more inter-polyplexes aggregates. Therefore, when short linear chains are used, the inter-polyplexes aggregation mainly follows the first pathway. On the other hand, Table 1 shows that for branched chains the dimer content (x) is less affected by their size. When a branched chain binds one of its sides to a segment of a DNA chain, it is unlikely that this DNA chain will be able to wrap itself tightly on such a branched chain with its neighboring segments because plasmid DNA chains are semirigid with a persistent length of ~50 nm. Instead, another side is more likely binds to another distant intrachain or interchain segment, i.e., condensing a DNA chain or bringing two DNA chains together. Therefore, when branched PEI chains are used, the polyplexes aggregate with each other most likely via the second pathway.

Table 1 also shows that for a given N/P ratio longer linear cationic PEI chains induce less inter-polyplexes aggregation than their shorter chain counterparts. Presumably, the imperfect alignment of longer linear chains on a DNA chain leads to the formation of small cationic loops and short brushes (tails) along the DNA chain. The charge neutralization results in the collapse of the DNA chain so that some of these cationic loops and tails stay on the periphery of each resultant polyplexes and stabilize them. In comparison with large branched chains, these small loops and short brushes are less effective in bridging two DNA chains together. On the other hand, when short linear PEI chains are used, the inter-polyplex aggregation gradually disappears as N/P increases, which is understandable because more cationic short chains are competing for each DNA chain and each PEI chain has a much less chance to align itself perfectly on it, especially its chain ends, so that a brush-like cationic coating is formed, stabilizing the resultant polyplexes. Figure 3 schematically summarizes the above discussion.

To further support our above argument, we measured the ratio of average radius of gyration ($\langle R_g \rangle$) and average hydrodynamic radius ($\langle R_h \rangle$) of the polyplexes prepared with different topologies, chain lengths and N/P ratios. This is because $\langle R_g \rangle / \langle R_h \rangle$ is related to the density distribution and compactness of a scattering object. For example, $\langle R_g \rangle / \langle R_h \rangle \sim 1.5$ for a narrowly distributed random-coiled chain, ~2 for an extended chain conformation, and ~0.774 for a uniform nondraining hard sphere.[31] Previous studies reported that for circular plasmid DNAs in a TE buffer $\langle R_g \rangle / \langle R_h \rangle$ is in the range

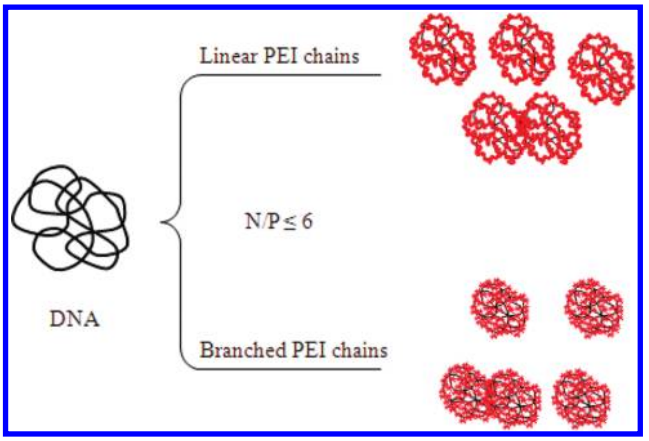

Figure 3. Schematic of complexation of DNA and PEI with different topologies in their solution mixtures when N/P is relatively low.

1.5−1.8, which is reasonable because plasmid DNA chains with a double-helix structure is semirigid with a persistent length (~50 nm).

Figure 4 shows that adding cationic PEI chains into a DNA solution leads to a dramatic decrease of its $\langle R_g \rangle / \langle R_h \rangle$ to 0.55−

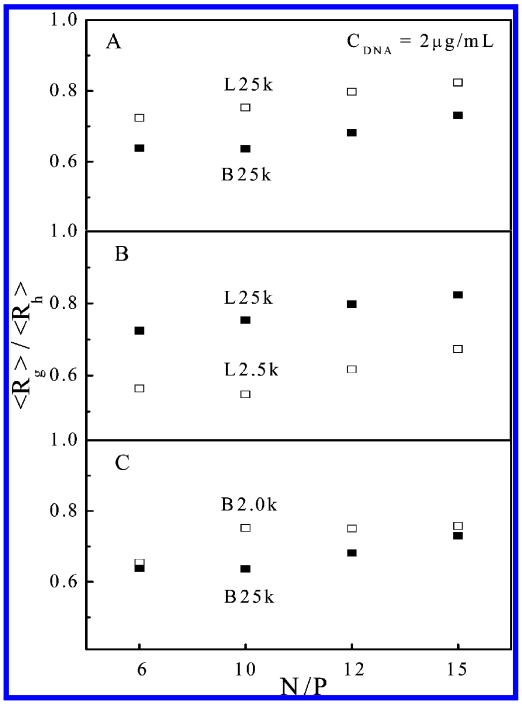

Figure 4. N/P ratio dependence of $\langle R_g \rangle / \langle R_h \rangle$ of polyplexes made of different PEI chains, where effects of (A) chain morphology: (B) and (C) chain length.

0.85, depending on the chain topology, length, and N/P ratio, much smaller than its value before the complexation. Such a change of $\langle R_g \rangle / \langle R_h \rangle$ shows the collapse of DNA chains and the formation of spherical-like polyplexes with a much higher chain density, similar to the collapse of linear neutral polymer chains in a very poor solvent. It is worth noting that especially at lower N/P ratios $\langle R_g \rangle / \langle R_h \rangle$ is even smaller than 0.774 predicted for a uniform hard sphere, indicating that the polyplexes have a core−shell structure with a less dense and partially draining periphery.[39] Presumably, for linear PEI chains, such smaller $\langle R_g \rangle / \langle R_h \rangle$ values can be attributed to the formation of small

dx.doi.org/10.1021/ma2027963 | Macromolecules 2012, 45, 4346−4353

loops and short tails on the periphery of each polyplexes, which increases its $\langle R_h \rangle$ but has a less effect on its $\langle R_g \rangle$; while for branched PEI chains, it is due to their sticking on the periphery of each polyplexes.

Moreover, $\langle R_g \rangle / \langle R_h \rangle$ always increases with N/P for a given DNA concentration because when more PEI chains are entrapped inside a polyplexes and attached on its periphery, it becomes more draining so that its $\langle R_h \rangle$ becomes smaller than its nondraining counterpart with a similar $\langle R_g \rangle$. In more details, Figure 4A shows that for a given molar mass long linear PEI chains generally lead to a larger $\langle R_g \rangle / \langle R_h \rangle$ than their branched counterparts, revealing that branched PEI chains lead to more compact and less draining polyplexes. This is because the imperfect annealing of a long linear PEI chain on a DNA chain inevitably results in some loops and tails that hinder further collapse of each DNA chain into a compact polyplexes.

Such an argument also explains why using shorter linear PEI chains leads to a smaller $\langle R_g \rangle / \langle R_h \rangle$ than using their longer counterparts, as shown in Figure 4B, in spite of different N/P ratios. Namely, a number of shorter linear PEI chains can align better on each DNA chain and neutralize its anionic charge so that both of PEI and DNA chains become insoluble and collapse in water to form more compact polyplexes stabilized by additional PEI chains anchored on their periphery. It also explains why the polyplexes made of short linear PEI chains are less stable and further aggregate with each other when there is no sufficient PEI chains in the solution mixture (N/P = 3), as shown in Figure 1.

Such a compactness difference between different polyplexes with only one DNA chain inside is more directly reflected in their size difference, as shown in Figure 5. Note that before the

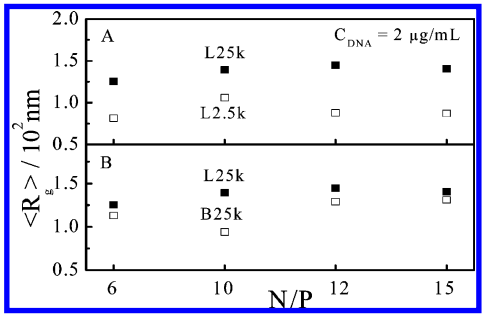

Figure 5. N/P ratio dependence of average radius of gyration ($\langle R_g \rangle$) of polyplexes, where effects of (A) chain length and (B) chain topology.

complexation in the presence of salt the DNA chains have an average hydrodynamic size of ~100−300 nm, depending on the salt concentration, aging time, and scattering angle used (one example is as shown in the Supporting Information). Please also note that supercoiled DNA plasmids should have a much longer persistent length than linear ones because two double helixes are further twisted together. Yoshikawa et al.[40] measured the size of supercoiled DNA plasmids (106 000 bp) and found that $\langle R_h \rangle \sim 940$ nm. Assuming that supercoiled DNA plasmids are rigid chains, we can scale down the Yoshikawa's result from 106 000 bp to our 5400 bp and find that $R_g \sim 210$ nm, not far away from our results in salt solutions.

In comparison, Figure 4C shows that using larger branched PEI chains only leads to a slightly smaller $\langle R_g \rangle / \langle R_h \rangle$ than using their smaller counterparts. Such a difference is also explainable because for a given N/P ratio the number of smaller chains is much more inside the solution mixture. Each larger branched PEI chain can bind different intrachain segments, acting as a cross-linker to pull different segments inside a DNA chain together to form a more compact structure, while a distribution of a number of smaller branched PEI chains on a DNA chain is just like to coat it with a layer of cationic charges, which prevents its further collapse so that their structure is less compact and more draining.

In either an *in vivo* or *in vitro* gene transfection experiment, DNA has to be wrapped and protected by a polymer vector to against the enzymatic degradation in both the extracellular and intracellular spaces. The condensation of DNA to small polyplexes is also a necessary condition for endocytosis (across the cell membrane). On the other hand, DNA has to be released from the polyplexes in the intracellular space so that the complexation (binding) between DNA and cationic polymer chains should not be too strong. Therefore, an optimal binding strength is critically important to balance different requirements. To test the binding strength of different PEI chains, we added anionic strong long polyanions (dextran sulfate, DS) into the solution mixture to see whether it can release anionic DNA inside the polyplexes.[6]

Figure 6A shows that before adding dextran sulfate into the solution mixture of DNA and PEI, the DNA chains are retarded

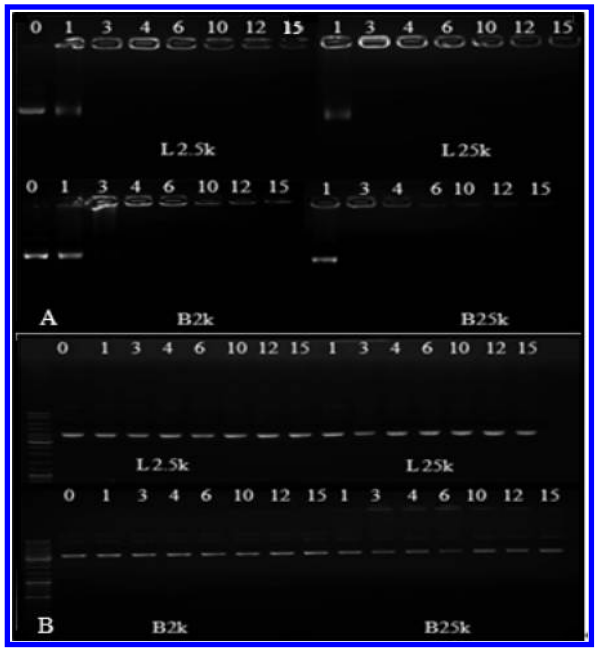

Figure 6. Gel electrophoresis of solution mixtures of L2.5k/DNA, L25k/DNA, B2.0k/DNA, and B25k/DNA at different N/P ratios, where (A) before and (B) after adding 50 times of dextran sulfate (weight ratio).

in the injection well during electrophoresis when N/P ≥ 3 because most of them are bound to PEI and condensed inside the polyplexes with a cationic periphery. On the other hand, Figure 6B shows that free DNA chains are clearly visible in electrophoresis after dextran sulfate is added except for those polyplexes made of large branched BPEI-25k chains, in which DNA chains are only partially released. Figure 6 shows that dextran sulfate can replace nearly all of the DNA chains inside the polyplexes made of PEI except for large branched chains. Further, we used the picogreen assay to quantitatively evaluate the extent of DNA released by dextran sulfate in each case

dx.doi.org/10.1021/ma2027963 | *Macromolecules* 2012, 45, 4346−4353

because its fluorescence intensity is correlated to the concentration of DNA segments that are not complexed with PEI.

Figure 7A shows that the fluorescence intensity of picogreen quickly decreases as more PEI chains are added in the range of

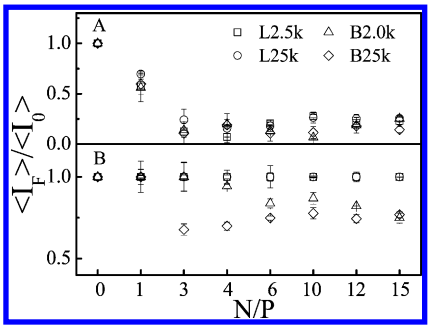

Figure 7. N/P ratio dependence of fluorescence intensity ($\langle I_F \rangle$) of picogreen in solution mixtures of DNA ad different PEI chains, where (A) before and (B) after adding 50 times of dextran sulfate (weight ratio); $\langle I_0 \rangle$ is fluorescence intensity of picogreen in pure DNA solution.

N/P $\leq$ 3, reflecting clear condensation of DNA by PEI, irrespective of its different topologies and chain lengths. Therefore, any release of DNA by dextran sulfate should increase the fluorescence intensity of picogreen. Figure 7B summarizes the relative picogreen fluorescence intensities of different solution mixtures of DNA and PEI, where each solution mixture contains 0.2 μg of DNA. After adding 10 μg of dextran sulfate, the fluorescence intensity of picogreen is fully recovered in most of the cases except when branched PEI chains are used. The partial recovery of the fluorescence intensity of picogreen in these solution mixtures reveals that not all of the DNA chains inside the polyplexes are released by dextran sulfate even if its weight concentration is 50 times more than that of DNA.

A combination of Figures 6 and 7 shows that branched PEI chains, especially larger ones, bind and protect DNA better than their linear counterparts. As discussed before, linear PEI chains can align themselves on a DNA chain and effectively neutralize its anionic charges so that they become insoluble and collapse in water to form compact polyplexes. In this case, only a fraction of free (non-neutralized) cationic amines remain on small PEI loops and tails due to some imperfect alignments. The added long anionic dextran sulfate chains can bind to those cationic groups on the periphery of each polyplexes and compete/replace with anionic DNA segments. The binding equilibrium shifts toward the complexation between PEI and dextran sulfate because of its higher concentration and strong electrolyte nature. After the peeling-off of the first layer of PEI, those DNA segments at the periphery become cationic and soluble so that they should extend into the solution mixture, leaving some open spaces for dextran sulfate to complex with inner PEI chains, similar to peeling an onion. Differently, besides their neutralization rule, branched PEI chains embedded inside each polyplexes bind and pull different intrachain segments together to form the polyplexes while those anchored on the periphery are only partially neutralized. It is those remaining cationic amines that stabilize each polyplexes. The peeling-off of those anchored PEI chains on the periphery makes the surface of each polyplexes becoming anionic and repelling anionic dextran sulfate so that further replacement of those branched PEI chains inside becomes more difficult.

CONCLUSION

The complexation of plasmid DNA and polyethylenimine (PEI) with different topologies and chains lengths results in small aggregates (polyplexes) in water, which was characterized by using a combination of static and dynamic laser light scattering. As expected, the polyplexes are instable and undergo further inter-polyplexes aggregation when the ratio of cationic amine (N) to anionic phosphate (P) is lower than 6. We found that at higher N/P ratios each polyplex on average contains only one DNA chain and has a sphere-like compact structure with a partially draining periphery made of small cationic PEI loops and tails or a layer of anchored cationic branched PEI chains. It is this cationic periphery that stabilizes individual polyplexes in water. Our study also uncovers that linear and branched PEI chains condense DNA in different ways. Namely, linear chains can align themselves on each DNA chain and more effectively neutralized its anionic charges so that their insolubility in water, just like hydrocarbon polymer chains, drives them into compact polyplexes. In contrast, each branched chain, besides its neutralization role, can bind different intrachain segments with its different sides to pull ("cross-link") them together to form compact polyplexes. It is due to such different condensation mechanisms that long anionic dextran sulfate chains can replace DNA from the polyplexes made of linear PEI chains but not those made of branched PEI chains, revealing that branched chains provide a better protection of DNA. The current study leads us to a better design of nonviral polymeric vectors for the gene transfection.

ASSOCIATED CONTENT

Supporting Information

Figures 1S and 2S. This material is available free of charge via the Internet at http://pubs.acs.org.

AUTHOR INFORMATION

Corresponding Author

*The Hong Kong address should be used for all correspondence.

Notes

The authors declare no competing financial interest.

ACKNOWLEDGMENTS

The financial support of the National Natural Scientific Foundation of China Projects (20934005 and 51173177), the Ministry of Science and Technology of China (Key Project, 2012CB933802), and the Hong Kong Special Administration Region Earmarked Projects (CUHK4042/10P, 2130241 and 2060405; CUHK4036/11P, 2130281 and 2060431) is gratefully acknowledged.

REFERENCES

(1) Pack, D.; Hoffman, A.; Pun, S.; Stayton, P. *Nat. Rev. Drug Discovery* **2005**, *4* (7), 581−593.
(2) Mintzer, M.; Simanek, E. *Chem. Rev.* **2009**, *109* (2), 259−302.
(3) De Smedt, S.; Demeester, J.; Hennink, W. *Pharm. Res.* **2000**, *17* (2), 113−126.
(4) Neu, M.; Fischer, D.; Kissel, T. *J. Gene Med.* **2005**, *7* (8), 992−1009.

(5) Lungwitz, U.; Breunig, M.; Blunk, T.; Gopferich, A. *Eur. J. Pharm. Biopharm.* **2005**, *60* (2), 247−266.
(6) Parhamifar, L.; Larsen, A.; Hunter, A.; Andresen, T.; Moghimi, S. *Soft Matter* **2010**, *6* (17), 4001−4009.
(7) Godbey, W.; Wu, K.; Mikos, A. *J. Biomed. Mater. Res.* **1999**, *45* (3), 268−275.
(8) Yue, Y.; Jin, F.; Deng, R.; Cai, J.; Chen, Y.; Wu, C. *J. Controlled Release* **2011**, 143−151.
(9) Ziebarth, J.; Wang, Y. *Biophys. J.* **2009**, *97* (7), 1971−1983.
(10) DeRoucheya, J.; Netz, R. R.; Radler, J. O. *Eur. Phys. J. E* **2005**, *16*, 17−28.
(11) Boussif, O.; Zanta, M.; Behr, J. *Gene Ther.* **1996**, *3* (12), 1074−1080.
(12) Morille, M.; Passirani, C.; Vonarbourg, A.; Clavreul, A.; Benoit, J. *Biomaterials* **2008**, *29* (24−25), 3477−3496.
(13) Ogris, M.; Steinlein, P.; Kursa, M.; Mechtler, K.; Kircheis, R.; Wagner, E. *Gene Ther.* **1998**, *5* (10), 1425−1433.
(14) Kircheis, R.; Kichler, A.; Wallner, G.; Kursa, M.; Ogris, M.; Felzmann, T.; Buchberger, M.; Wagner, E. *Gene Ther.* **1997**, *4* (5), 409−418.
(15) Fischer, D.; Bieber, T.; Li, Y.; Elsasser, H.; Kissel, T. *Pharm. Res.* **1999**, *16* (8), 1273−1279.
(16) Wightman, L.; Kircheis, R.; Rossler, V.; Carotta, S.; Ruzicka, R.; Kursa, M.; Wagner, E. *J. Gene Med.* **2001**, *3* (4), 362−372.
(17) Han, J.; Kim, S.; Cho, T.; Lee, J.; Joung, H. *Macromol. Res.* **2004**, *12* (5), 501−506.
(18) Choosakoonkriang, S.; Lobo, B.; Koe, G.; Koe, J.; Middaugh, C. *J. Pharm. Sci.* **2003**, *92* (8), 1710−1722.
(19) Ketola, T.; Hanzlikova, M.; Urtti, A.; Lemmetyinen, H.; Yliperttula, M.; Vuorimaa, E. *J. Phys. Chem. B* **2011**, *115* (8), 1895−1902.
(20) Ogris, M.; Brunner, S.; Schuller, S.; Kircheis, R.; Wagner, E. *Gene Ther.* **1999**, *6* (4), 595−605.
(21) Kircheis, R.; Schuller, S.; Brunner, S.; Ogris, M.; Heider, K.; Zauner, W.; Wagner, E. *J. Gene Med.* **1999**, *1* (2), 111−120.
(22) Erbacher, P.; Bettinger, T.; Belguise-Valladier, P.; Zou, S.; Coll, J.; Behr, J.; Remy, J. *J. Gene Med.* **1999**, *1* (3), 210−222.
(23) Boeckle, S.; von Gersdorff, K.; van der Piepen, S.; Culmsee, C.; Wagner, E.; Ogris, M. *J. Gene Med.* **2004**, *6* (10), 1102−1111.
(24) Wagner, E.; Cotten, M.; Foisner, R.; Birnstiel, M. *Proc. Natl. Acad. Sci. U. S. A.* **1991**, *88* (10), 4255−4259.
(25) Kunath, K.; von Harpe, A.; Fischer, D.; Peterson, H.; Bickel, U.; Voigt, K.; Kissel, T. *J. Controlled Release* **2003**, *89* (1), 113−125.
(26) Godbey, W.; Wu, K.; Mikos, A. *Proc. Natl. Acad. Sci. U. S. A.* **1999**, *96* (9), 5177−5181.
(27) Pollard, H.; Remy, J.; Loussouarn, G.; Demolombe, S.; Behr, J.; Escande, D. *J. Biol. Chem.* **1998**, *273* (13), 7507−7511.
(28) Itaka, K.; Harada, A.; Yamasaki, Y.; Nakamura, K.; Kawaguchi, H.; Kataoka, K. *J. Gene Med.* **2004**, *6* (1), 76−84.
(29) Dai, Z.; Gjetting, T.; Mattebjerg, M. A.; Wu, C.; Andresen., T. L. *Biomaterials* **2011**, *32* (33), 8626−34.
(30) Teraoka, I. *Polymer Solution: An Introduction to Physical Properties*; John Wiley & Sons, Inc.: New York, 2002.
(31) Chu, B. *Laser Light Scattering*; Acdemic Press: New York, 1974.
(32) Pecora, R. *Dynamic Light Scattering: Application of Photon Correlation Spectroscopy*; Plenum Press: New York, 1985.
(33) Provencher, S. *Makromol. Chem., Macromol. Chem. Phys.* **1979**, *180* (1), 201−209.
(34) Choosakoonkriang; Lobo, B.; Koe, G.; Koe, J.; Middaugh, C. *J. Pharm. Sci.* **2003**, *92* (8), 1710−1722.
(35) Von Harpe, A.; Petersen, H.; Li, Y.; Kissel, T. *J. Controlled Release* **2000**, *69* (2), 309−322.
(36) Liang, D.; Luu, Y.; Kim, K.; Hsiao, B.; Hadjiargyrou, M.; Chu, B. *Nucleic Acids Res.* **2005**, *33* (19), e170.
(37) Fluegel, S.; Maskos, M. *Biomacromolecules* **2007**, *8* (2), 700−702.
(38) Storkle, D.; Duschner, S.; Heimann, N.; Maskos, M.; Schmidt, M. *Macromolecules* **2007**, *40*, 7998−8006.
(39) Wu, C.; Zhou, S. *Phys. Rev. Lett.* **1996**, *77* (14), 3053−3055.
(40) Araki, S.; Nakai, T.; Hizume, K.; Takeyasu, K.; Yoshikawa, K. *Chem. Phys. Lett.* **2006**, *418*, 255−259.